5
PULSE-FORMING NETWORKS

As was pointed out in Chapter 3, the line-type modulator uses an energy-storage element that is similar to an open-circuited transmission line. There are some applications where actual lengths of transmission line are utilized for this element, but this normally is done only for short pulse lengths because of the size and inconvenience of the line length required for longer pulses. In addition, the use of an actual transmission line has other disadvantages, namely its lack of flexibility and inability to adjust for nonideal circuit elements.

In order to circumvent these disadvantages, lumped constant networks are normally utilized rather than actual transmission lines. When line-type modulators were first developed, attempts were made to simulate the transmission line by using the equivalent derived by Rayleigh; however, no matter how many sections were used, overshoots and ringing still existed at the front and leading edges of the output pulse. The reason for these oscillations is Gibbs' phenomenon, associated with the nonuniform convergence of a Fourier series near the discontinuity of a rectangular output pulse. Guillemin realized this difficulty and derived a set of networks that approximate a trapezoidal pulse with nonzero rise and fall time [8]. A number of these networks are summarized in Figure 5–1. One particularly convenient form of the pulse-forming network is the so-called Guillemin E-type network, which has equal-value capacitors and a continuously wound tapped coil whose physical dimensions are chosen so as to provide the proper mutual coupling between tapped sections. The total capacitance and inductance are given by the equations

$$C_n = \frac{\tau}{2Z_o} \tag{5-1}$$

$$L_n = \frac{\tau Z_o}{2} \tag{5-2}$$

where τ = output pulse width
Z_o = characteristic impedance

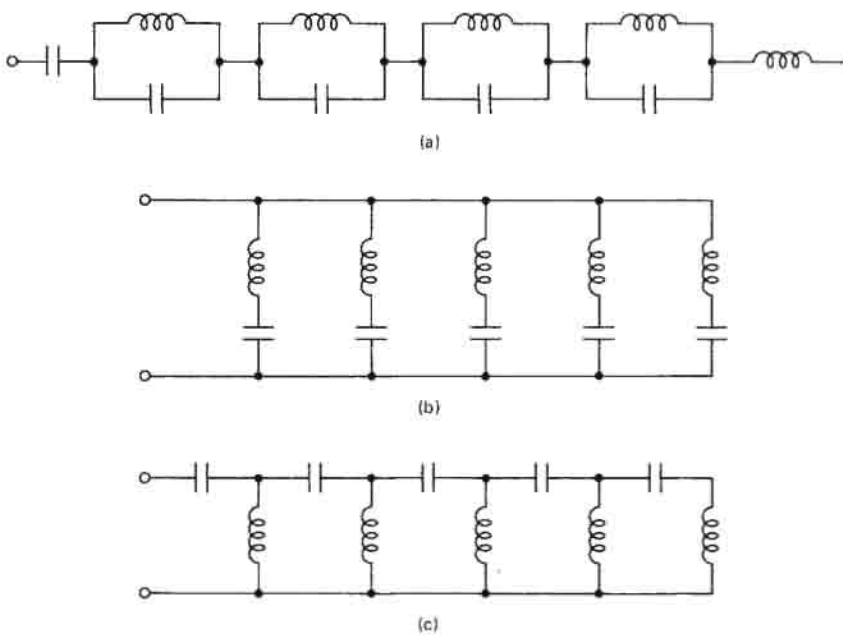

FIGURE 5–1 Some possible, but not rarely used, forms of PFNs: (*a*) type A, (*b*) type C, (*c*) type F.

The number of sections is chosen to provide the desired rise time. The design equations for such a network are summarized in Figure 5–2.

5–1 PFN DESIGN

The design of an E-type voltage-fed Giullemin network [3,4,8] is begun by specifying the number of sections in the network, the impedance of the network, and the pulse width of the network. The pulse width and impedance level are usually specified in the general design

Important relations are:

$$Z_o = \sqrt{\frac{L_n}{C_n}}$$

$$\tau = \sqrt{L_n C_n}$$

$$C_n = \frac{\tau}{2Z_o}$$

$$L_n = \frac{\tau Z_o}{2}$$

$$\frac{l}{d} = \frac{4}{3}$$

$$\frac{L_c}{L} = 1.1 \text{ to } 1.2$$

where C_n = total network capacitance
L_n = total network inductance
τ = pulse width at 50% points
Z_o = characteristic impedance
n = number of sections
L = inductance per section L_n/N
L_c = inductance of section on closed end
C = capacitance per section C_n/n
l = length of coil in one section
d = coil diameter

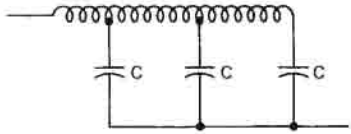

FIGURE 5–2 Guillemin E-type pulse-forming network circuit diagram and critical design parameters.

of the modulator. The number of sections desired is less evident and depends on many factors. For a more complete discussion, see Gillette and Oshima [7].

When PFNs are used to pulse a magnetron through a pulse transformer, the following guideline may be used:

Number of sections	Pulse length
1–3	Less than 0.5 μs
2–5	0.5–2.5 μs
3–8	2.5–5.0 μs

These usually give reasonably good results and generally agree with the results obtained by the methods in Gillette and Oshima [7].

If it is necessary to achieve a specified rise time, the number of sections is given by

$$\frac{0.63\tau}{t_r} + 0.13$$

where τ is the pulse width at the 70% level and t_r the rise time from 10% to 90%. Now we may calculate C_n and L_n using Equations 5–1 and 5–2, and use the design equations given in Figure 5–2.

5–2 COIL DESIGN

The PFN inductor design requires the calculation of a close-wound coil having a length/diameter ratio of 4/3 per section (for close-wound coils having more than one section) and a total inductance L_n. The ratio of length to diameter for single-section coils is not critical.

The "current sheet" inductance of a solenoid is given in Langford-Smith [12] as

$$L_n = \frac{0.1\ a^2 N^2}{l\ K}$$

where L_n = inductance μH
a = radius of coil (in)
N = number of turns
l = length of coil (in)
K = Nagaoka's constant

or

$$N = \left[\frac{10 L_n\ l}{a^2 K}\right]^{1/2} \tag{5–3}$$

Values of Nagaoka's constant are

Number of sections	Diameter/length	Nagaoka's constant
1	Any	As appropriate
2	0.375	0.86
3	0.25	0.91
4	0.137	0.925
5	0.15	0.94

A usual procedure would be to select a standard-size coil form and then to calculate the length of the coil. Then the number of turns may be calculated. By using a 90% winding-space factor, the allowable wire size may now be calculated. The power dissipated in the wire should now be checked (remember that the pulse current flows only on the inner half of the wire). If the coil is space-wound, Equation 5–3 may be somewhat in error and more exact expressions will be required [12]; however, this is usually not necessary.

Taps are placed at approximately the following places on the coil:

	Tap location (% of total turns)				
Number of sections	1	2	3	4	5
2	60	100			
3	39	68	100		
4	30	52	74	100	
5	25	43	61	79	100

There should be provisions to adjust the position of each coil tap to optimize pulse shape.

For extremely high voltage (pulse voltage greater than 10 kV), it will be necessary to space-wind the coil. For extremely long-pulse coils, bank winding may be convenient. In these cases, the methods given in "Colloquium on PFN's" [4] are appropriate.

There are, of course, a number of networks that have been designed for specific applications to generate unusual waveshapes [3,19].

5–3 VOLTAGE-MULTIPLYING NETWORKS

There are a number of voltage-multiplying networks that can be utilized to increase the output voltage from a discharge pulse generator without the use of a pulse transformer. The simplest of these is the Marx generator, shown in Figure 5–3, consisting of a number of capacitors charged in parallel but discharged in series.

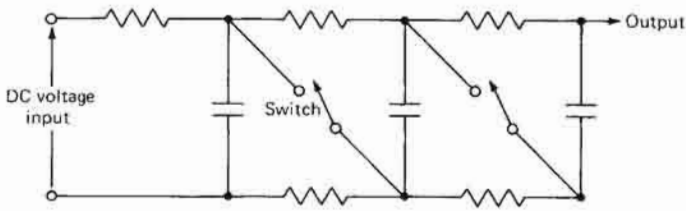

FIGURE 5–3 Marx circuit for generation of high-voltage impulses.

More control over the pulse shape may be obtained by a so-called Darlington line, shown as Figure 5–4, for which the various sections satisfy the relationship that for an n-network system, the impedance of the rth network is

$$Z_r = \frac{R_l r(r+1)}{n^2}$$

and the impedance of the nth network is

$$Z_n = \frac{R_l}{n}$$

The voltage of the output pulse is $n/2$ times the network voltage. The particular case where the Darlington line consists of two sections is called a *Blumlein network;* it is shown as Figure 5–5.

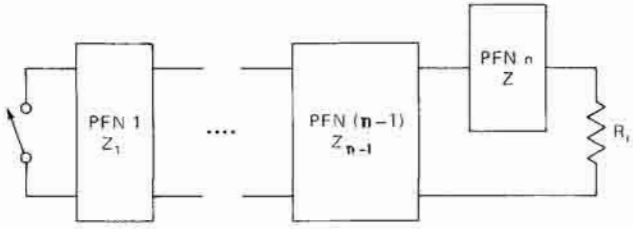

FIGURE 5–4 Block diagram of a Darlington line.

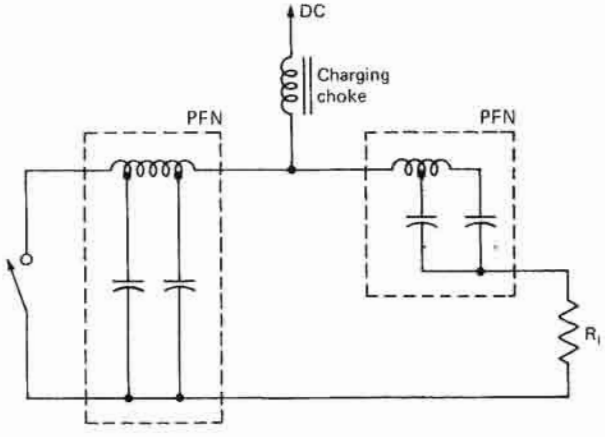

FIGURE 5–5 Blumlein circuit.

5–4 PULSE CAPACITORS

The pulse capacitors in a Guillemin E-type PFN are all of equal value; that value is C_n/n. These capacitors must satisfy a number of different criteria, including having low internal inductance and high stability and being able to withstand high applied voltages and to function reliably for extended periods of time at high recharge and discharge rates.

The design of ac and pulse capacitors involves many factors, a number of which are not clearly understood, and few general statements can be made [2,6,11,16,18]. There are many factors that affect the life of a capacitor in pulse service. These include failure due to corona in the capacitor structure, actual burning of the insulation, deterioration of the insulation due to excessive heat, and failure due to harmful chemicals attacking the dielectric. Obtaining specific information on any portion of the capacitor design or construction process is relatively difficult, and most successful designs are based on extrapolation from earlier known cases.

It has been empirically observed that if the voltage across a single capacitor section exceeds some critical value, it will be very difficult to prevent damaging corona from occurring. For this reason, in a five-section, 1-μs network described in Glasoe and Lebacqz [8], Sprague used four series-connected sections worked at 2 kV peak charging voltage per section. The paper dielectric in each section was stressed at about 210 V/mil. In a four-section, 1.8-μs network charging to 15.2 kV and required to stand 30.4 kV peak charging for 24 h, each section consisted of twelve series-connected capacitors, so that each section was worked 1250 V (2500 V for the 24-h test), with the dielectric (Samica, reconstituted mica paper) worked at about 705 V/mil and stressed at 1410 V/mil for the 24-h test at twice working voltage [15]. Another paper capacitor had 14 series-connected sections for 13.2 kV peak charging voltage, inserted tab construction, and an insulation of five layers of 0.5-mil paper. This resulted in a voltage per section of 950 V, with the insulation stressed at 380 V/mil. A design with 16 kV peak charging voltage had three wound capacitors in series with two floating foils in each section. Insulation was 12 layers of 0.5-mil paper for each section, resulting in a stress per section of 1777 V, with the insulation stressed at 300 V/mil [14]. AMP, Inc., has constructed a network having a peak charging voltage of 10 kV in which each capacitor consists of two series-connected Isomica capacitor sections, with a resulting stress of 5 kV per section [1].

A theoretical basis for the division of high-voltage ac and pulse capacitors into a number of series-connected sections may be found by considering the behavior of laminar voids in the insulation. Consider the situation shown in Figure 5–6, with a laminar void in the insulation between two conductors, or capacitor plates. For electric fields perpendicular to the insulator surface, the stress in volts per mil in the gas constituting the void is equal to the electric field in the insulator multiplied by the dielectric constant of the solid material, assuming that the dielectric constant of the void is 1.0.

For example, if the stress in an insulator of dielectric constant 4.0

is 50 V/mil, the stress in the air between it and the nearby conductor may be as high as 200 V/mil. Since, in general, the gas is the material with the lower breakdown voltage, it will break down at a total applied voltage that the solid dielectric material can easily support.

The voltage across the combination of insulator and void at which incipient breakdown will occur in the voids has been determined by

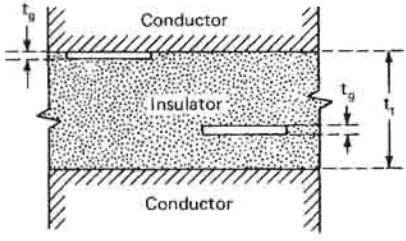

FIGURE 5–6 Idealized voids in solid insulation between two conductors. [17]

Olyphant [17]. For the case of Figure 5–6, assume that a voltage V_t is applied between the electrodes and is given by the sum of the voltage V_g across the gas and V_x across the solid,

$$V_t = V_g + V_x$$

or

$$V_t = E_g t_g + Et$$

where E_g and E are the stresses in the gas and the solid and t_g and t are their respective thicknesses. Thus,

$$V_t = E_g\left(t_g + \frac{t}{k}\right)$$

where k is the dielectric constant of the solid material.

If E_g is set equal to the breakdown strength of the gas, V_t becomes the corona starting voltage, or the voltage at which breakdown first occurs in the laminar void. This corona start voltage has been found to be relatively independent of frequency over the range from 60 Hz to above 1 MHz.

If the values of breakdown strength as a function of air gap at atmospheric pressure are substituted for E_g, a family of curves of corona starting voltage is obtained. Such a family is shown in Figure 5–7. For any value of t/k there is an air gap in which discharges will first occur, and which will give a minimum corona starting voltage. The minimum values of corona starting voltage obtained from Figure 5–7 are replotted as

Figure 5–8. Also shown in Figure 5–8 is a plot of values estimated from Figure 5–7 for the air gap spacing in which discharges will first occur. These spacings are not particularly critical, since corona starting voltage does not vary rapidly with changes in spacing near the minimum.

Approximations for both the minimum corona starting voltage in

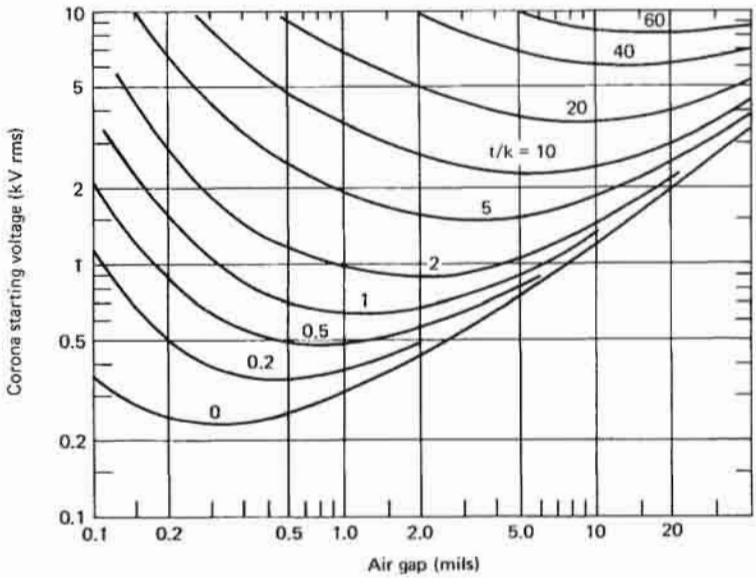

FIGURE 5–7 Calculated corona starting voltages in laminar voids at atmospheric pressure as a function of the void spacing (air gap) for various values of effective insulation thickness (t/k). [17]

laminar voids and the gap for minimum corona starting voltage are given by the following fitted equations:

$$\text{CSV} = 0.56 \left(\frac{t}{k}\right)^{0.61} \text{(kV rms)}$$

$$t_g = 1.25\ (t/k)^{0.67} \text{ (mil)}$$

Thus, one can see that for a minimum-volume capacitor, series connections of individual capacitors are desirable, with voltage per section limited to less than from 2 to 4 kV.

The physical design of pulse capacitors must be such that the self-inductance of the capacitors is minimized. In long-pulse units (where lead inductance is not as important), inserted-tab construction is often used if the resulting high-current densities do not cause excessive local

heating. Generally a thin piece of some solderable material is inserted into the capacitor to contact the aluminum capacitor foils. While there is only a pressure contact and dissimilar metals are used, both nickel and tin-plated copper have been successfully used as tabs in the capacitor industry. For shorter-pulse-length units, the entire edge of each foil

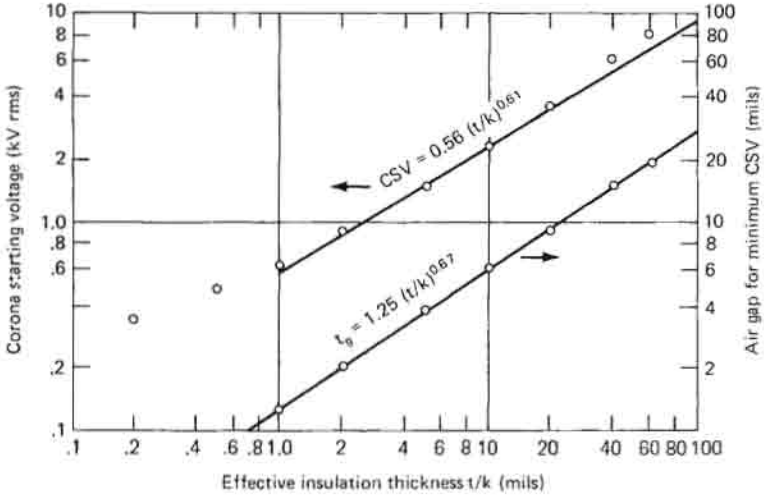

FIGURE 5–8 Minimum corona starting voltage (CSV) as a function of effective insulation thickness. Air-gap spacings for minimum corona starting voltage are also shown. [17]

must be contacted, and the result is either the extended-foil capacitor or the wafer capacitor. The extended-foil capacitor merely extends the foils beyond the edge of the capacitor insulation. The connection is made to the aluminum foil after impregnation of the capacitor. A tin-lead-zinc solder and *no flux* is used to make the solder connection [14]. The solder is applied with a wiping motion of the iron, abrasion alone being used to clean the surface of the aluminum foil. The resulting joint is not very pretty, but it seems to be adequate. Since such techniques are quite expensive, they are usually reserved for exacting applications.

There is no question that the presence of corona does deteriorate the insulation in a capacitor. Also, for otherwise identical capacitors, the one with less corona will usually have the longer life. The correlation between corona levels and life expectancy among *different* capacitors, even those using the same dielectric and impregnants, is rather poor, and corona testing by itself is a poor way to predict capacitor life. For a more extensive discussion of corona testing, see Birks and Schulman [2] and Kreuger [11].

One dielectric that is quite resistant to corona effects is reconstituted mica paper, which is available in several forms. One form that is particularly useful for low-volume pulse capacitors is Isomica, a stage-B resin-impregnated reconstituted mica paper. AMP, Inc., is using capacitors of Isomica to replace its Amplifilm capacitors at high PRFs and high temperatures, and Isomica capacitors are also manufactured by Sprague, Tobe, and Custom. The Isomica is relatively cheap, the capacitors are fairly easy to make, and the Isomica is very heat- and corona-resistant.

Capacitors made from Isomica are stacked-wafer capacitors. The capacitors are stacked and placed in a press, and about 1000 lb/in^2 of pressure is applied and the temperature is raised to 300°C as rapidly as possible while pressure is still maintained. The capacitor is baked for 20 h at 300°C and 1000 lb/in^2, and is then cooled and removed from the press and postbaked for 48 h at 150°C [10,21]. After baking, the capacitor must be kept extremely dry, for it absorbs moisture readily. One easy way to do this is to place the capacitor in a mason jar with a desiccant during the postbake and put the lid on the jar while still hot.

The dielectric stress used by commercial companies is one 2-mil sheet of Isomica for each 1000 V of peak charging voltage, with a maximum of 5 to 8 kV per capacitor section. In capacitors constructed at Georgia Tech, about half that stress has been used. The finished capacitors have excellent resistance to heat, many having been operated at 175°C with no ill effects. The capacitors should always be cased and the cases thoroughly impregnated and sealed to prevent absorption of moisture. Suitable impregnants include silicone oil and transformer oil. If desired, wrap and end-fill techniques may be used to exclude moisture.

Because of the difficulties of implementing large capacitances in a stacked-capacitor configuration, and because of limited demand, Isomica has been largely replaced by Samica, which is an unimpregnated reconstituted mica paper. Samica may be used to make wound capacitors by conventional techniques; aluminum-foil electrodes and inserted-tab construction are often used. After winding, the capacitor is normally vacuum-dried and then impregnated. If the capacitor is to be sealed and liquid-impregnated, normally silicone or mineral oils will be used. If a dry capacitor is desired, the capacitor may be impregnated with either a liquid polyester or an epoxy compound and then cured under heat and pressure to produce the finished capacitor. Typical capacitance stability will be better than ±2% from −55 to +105°C, with a dissipation factor less than 0.005 at 25°C and less than 0.008 at +125°C.

5–5 TEMPERATURE-RISE CALCULATIONS

The temperature rise of a pulse-forming network is related to the total energy per pulse and the number of pulses per second passed

through the pulse-forming network. Thus, a measure of the losses in watts for a particular type of pulse-forming network is

$$\frac{1}{2} C_n V^2 f$$

where C_n = PFN capacitance
f = PRF

and

V = peak network voltage

and this fact has been used to provide guidelines for initial estimation of case sizes by Graydon [9]. These procedures are summarized below, and can serve as a first estimate for case size selection for both paper and mica capacitors.

Graydon's procedures for case size (or area) selection involve calculating a number of normalized parameters and entering a standard curve. If the parameters

τ = PFN pulsewidth (s)
Z_o = characteristic impedance of PFN (Ω)

and the maximum ambient temperature is known, the case selection may be accomplished by the following steps:

1. Calculate $C_n = \tau/2Z_o$.
2. Calculate $(1/2)C_n V^2 f$.
3. Calculate C_1 equal to maximum ambient temperature less 20°C.
4. Calculate $C_2 = 31\left(\frac{1}{2} C_n V^2 f\right)^{0.4}$ (Figure 5–9 may be used).
5. Enter Figure 5–9 to determine the life factor $F(H)$.
6. Calculate

$$C_4 = \frac{K_a F(H)}{0.001[(\frac{1}{2})C_n V^2 f]V\sqrt{C_n}}$$

For K_a use 0.035 for V below 15 kV, 0.025 above 20 kV, and 0.0275 above 25 kV.

7. Calculate $Y = AC_2/C_4$ (see Table 5–1 for A).
8. Calculate $X = BC_1/C_4$ (see Table 5–1 for B). Using the calculated value of Y, enter Figure 5–10 and determine case area

from the intersection of the calculated Y value and the line corresponding to the calculated value of X.

9. Enter Figure 5–10 to determine case size.

This case area is a preliminary estimate, and more detailed calculations are normally required to determine exact temperature rise. However,

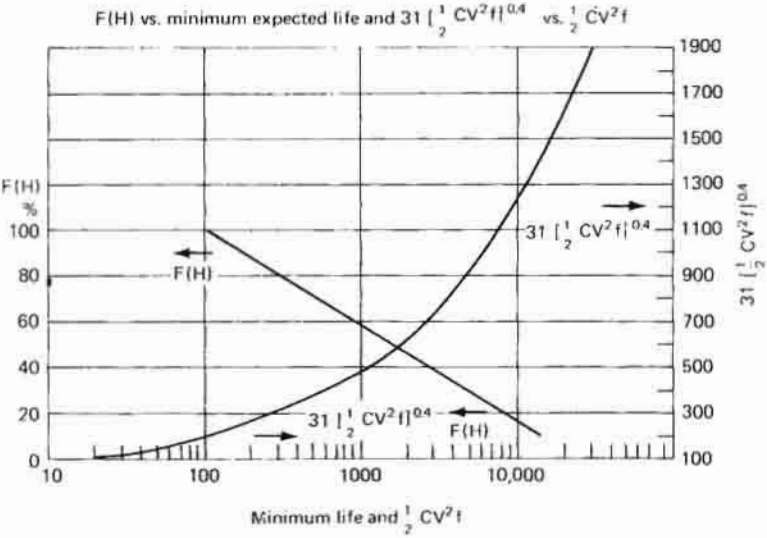

FIGURE 5–9 Guide curves for Figure 5–10. [9]

in a more detailed consideration, individual losses in the various components must be carefully calculated. The principal sources of loss in a pulse-forming network are losses in the capacitor, losses in the coil, and losses in the can itself due to currents induced by the PFN coil. Except for the highest-powered networks, a calculation of losses in the capacitor and in the coil will be sufficient.

Coil losses may be calculated by utilizing the effective wire resistance, which was discussed earlier (Equation 4–2), and by assuming that current flows in only the inner portion of the coil because of proximity effects. The use of litz wire may be somewhat beneficial in reducing the magnitude of these coil losses.

Calculation of the losses in the capacitors may proceed along several distinct lines. The simplest and least accurate approach is to utilize a gross dissipation factor between 0.005 and 0.01 and multiply $(\frac{1}{2})CV^2f$

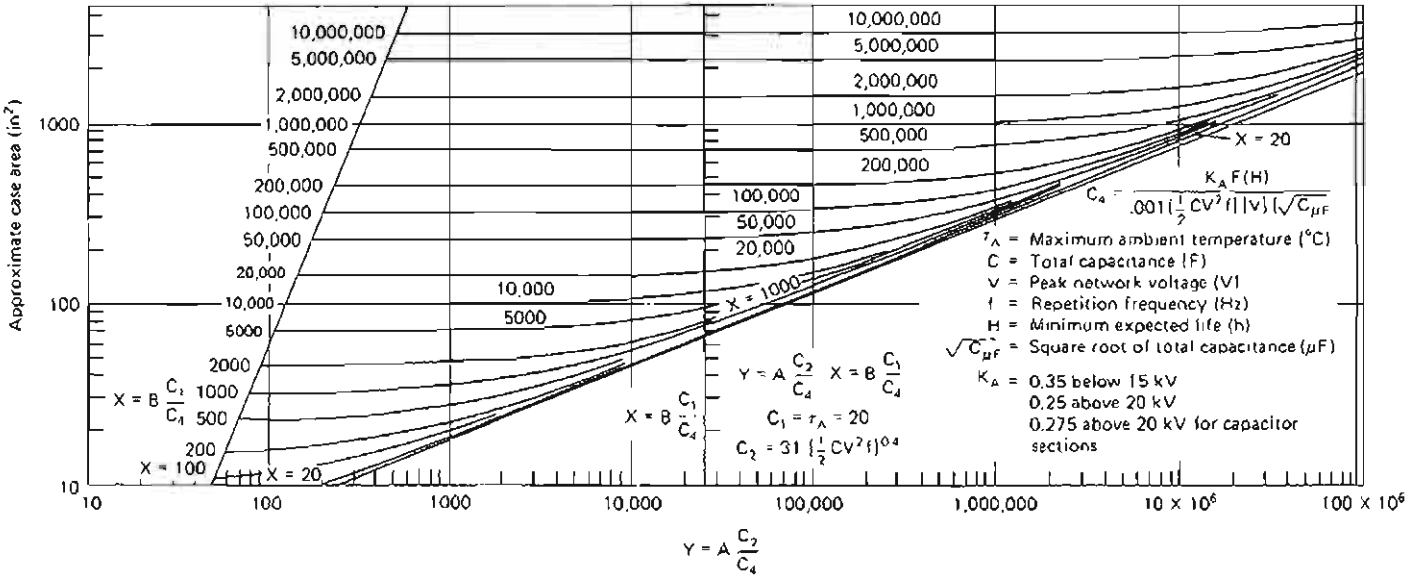

FIGURE 5–10 Estimated PFN case area as a function of known parameters. [9]

TABLE 5–1 COEFFICIENTS OF C_2/C_4 AND C_1/C_4 [9]

Circulation construction	C_2/C_4 coefficient A	C_1/C_4 coefficient B
Natural circulation, internal coil, no fins, no forced air	1	1
Internal coil, either fins or forced air at 400 ft/min	0.38	0.50
Both fins and forced air at 400 ft/min, internal coil	0.215	0.333
Natural circulation, external coil (capacitor section), no fins, no forced air	0.38	0.50
Either fins or forced air at 400 ft/min, external coil (capacitor section)	0.215	0.333

by the dissipation factor to obtain total capacitor losses. However, in higher-power networks, the procedure advocated by Lerner [13] or by Rambo and Gardenghi [20] will usually be required, involving calculation of the Fourier components of the voltage waveforms applied to the capacitor, and the determination of the heating associated with each of these components.

Because of uncertainties in many aspects of PFN temperature-rise calculations, capacitor-loss calculations should be carefully checked experimentally to ensure their correctness. Fortunately, some types of PFN capacitors are used in sufficient quantities that extensive experience is available, permitting quite accurate procedures for estimates of capacitor losses to be developed. One such procedure has been developed by Custom Electronics for use with its wrap-and-fill mica capacitors [5]. For these capacitors, the losses in the capacitor are given by

$$\frac{1}{2} I^2 C f \times \mathrm{DF}$$

where V = peak network charging voltage
C = capacitance
f = PRF

and the dissipation factor (DF) is a function of pulse width, number of PFN meshes, and PRF. One table for finding DF is Table 5–2.

Once these various PFN losses have been calculated, the temperature-rise calculations outlined in Chapter 4 are completely applicable.

TABLE 5–2 DISSIPATION FACTOR AS A FUNCTION OF PRF AND F, THE RATIO OF NUMBER OF PFN SECTIONS TO PULSE WIDTH, FOR WRAP-AND-FILL RECONSTITUTED MICA CAPACITORS [5]

	Dissipation factor (DF) for various values of F				
PRF	4.0×10^6	6.0×10^6	8.0×10^6	12.0×10^6	16.0×10^6
500	0.020	0.021	0.022	0.024	0.026
1000	0.021	0.022	0.023	0.025	0.027
1500	0.022	0.023	0.024	0.026	0.028
2000	0.023	0.024	0.025	0.027	0.029
2500	0.024	0.025	0.026	0.028	0.030
3000	0.025	0.026	0.027	0.029	0.031
3500	0.026	0.027	0.029	0.030	0.032
4000	0.027	0.028	0.029	0.031	0.033

REFERENCES

1. Ahern, Jack, AMP, Inc., personal communication.

2. Birks, J. B., and J. H. Schulman, eds., *Progress in Dielectrics*, vol. 1, Heywood and Company, Ltd., London, 1959, pp. 5–8, 19–31.

3. "Calculation of PFN's Having Slow Rates of Rise," MIT Radiation Laboratory Report 698, Cambridge, Mass., Mar. 12, 1945.

4. "Colloquium on PFN's," MIT Radiation Laboratory Report 692, Cambridge, Mass., Mar. 14, 1945.

5. Custom Electronics technical staff, "Heat Dissipation and Other Considerations in Custom Electronics' Type "C" Reconstituted Mica Capacitors Used in Pulse Forming Networks," Custom Electronics, Inc., Oneonta, N.Y., August 1978.

6. Drummer, G. W. A., and H. M. Nordenberg, *Fixed and Variable Capacitors*, McGraw-Hill, New York, 1960.

7. Gillette, P. R., and K. Oshima, "Pulser Component Design for Proper Magnetron Operation," *IRE Trans. Component Parts*, vol. CP-3, no. 1, March 1956, pp. 26–31.

8. Glasoe, G. N., and J. V. Lebacqz, *Pulse Generators*, MIT Rad. Lab. series, vol. 5, McGraw-Hill, New York, 1948, pp. 215–221, 655–660. (Also available in Dover and Boston Technical Publishers editions.)

9. Graydon, A., "The Application of Pulse-Forming Networks," *IRE Trans. Component Parts*, vol. CP-4, no. 1, March 1957, pp. 7–13.

10. Hogle, D. H., "Samica/Isomica Dielectrics for Capacitors," *Electrical Shorts*, 3M Company, no. E-PRES-12-1 (45.5) BPH. St. Paul, Minn.

11. Kreuger, F. H., *Discharge Detection in High Voltage Equipment*, American Elsevier, New York, 1965.

12. Langford-Smith, F., ed., *Radiotron Designer's Handbook*, 4th ed., distributed by RCA, Harrison, NJ, 1953, pp. 429–432.

13. Lerner, M., "Which Non-Sinusoidal Voltage May Shorten the Life of a Capacitor?" in *Proc. 1977 Electronic Components Conf.*, pp. 468–474.

14. Lord, Richard, Sprague Electric Company, personal communication.

15. Lord et al., "Development of High Temperature Pulse Forming Network," Final Report, Sprague Electric Company, AD No. 285–305, North Adams, Mass., July 30, 1962.

16. Mabury, R. E., *Power Capacitors*, McGraw-Hill, New York, 1949, pp. 29–38.

17. Olyphant, M., Jr., "Corona and Treeing Breakdown of Insulation: Progress and Problems," pt. I, *Insulation*, vol. 9, February 1963, pp. 35–40.

18. Parkman, N., "Some Properties of Solid-Liquid Composite Dielectric Systems," *IEEE Trans. Electrical Insulation*, vol. EI-13, no. 4, August 1978, pp. 289–307.

19. Perry, A. D., "Pulse-Forming Networks Approximating Equal-Ripple Flat Top Step Response," in *IRE Nat. Conv. Rec.*, vol. 5, 1957, pp. 148–153.

20. Rambo, S. I., and R. A. Gardenghi, "PFN Loss Calculations," in *1978 13th Pulse Power Modulator Symp.*, pp. 43–45.

21. 3M Company, *Processing Instructions for Isomica Capacitors.*